Journal of
Ceramic Science
and Technology

J. Ceram. Sci. Technol., **15** [1] 49-54 (2024)
DOI: 10.4416/JCST2023-00013
available online at: http://www.ceramic-science.com

Short Communication

Characterization and Dielectric Behavior of Varied Sintering-Accelerator-Doped Magnesium Titanates at Microwave Frequency

C.-H. Shen*

Department of Electronic Engineering, Ming Chuan University, 5 De Ming Rd., Gui Shan District, Taoyuan City 333, Taiwan

received September 19, 2023; received in revised form November 22, 2023; accepted December 12, 2023

Abstract

To lower the phase-forming temperature of magnesium titanate, $MgTiO_3$, magnesium ions were replaced with 0.05 mole of cobalt ions and diverse low-melting-point materials were as sintering accelerators. The phase formation of $0.9Mg_{0.95}Co_{0.05}TiO_3 - 0.1Ca_{0.61}Nd_{0.78/3}TiO_3$ dielectric ceramics was verified by means of XRD diffraction to observe the crystallites of varied phases. SEM was used to observe the particle growth of the ceramic system and the composition ratio of the particles was analyzed by means of EDS. In contrast with the pure $0.9Mg_{0.95}Co_{0.05}TiO_3 - 0.1\ Ca_{0.61}Nd_{0.78/3}TiO_3$ dielectric ceramics, the results show that the sintering temperature can be effectively decreased. The microwave dielectric performances of $0.9Mg_{0.95}Co_{0.05}TiO_3 - 0.1Ca_{0.61}Nd_{0.78/3}TiO_3$ dielectric ceramics are closely related to the density and the growth of particles in the specimens. When 0.25 wt% V_2O_5 were added to the $0.9Mg_{0.95}Co_{0.05}TiO_3 - 0.1\ Ca_{0.61}Nd_{0.78/3}TiO_3$, the dielectric ceramics showed an ε_r value of 21.7, a Qf value of 71 000 GHz, and a τ_f value of -22.7 ppm/K, while the sintering temperature was reduced from 1 350 °C to 1 250 °C (that is about 100 °C). The results are almost identical for the different accelerators, but some of them have a more significant negative effect on the dielectric performance.

Keywords: Dielectric ceramics, low melting point, phase formation, microwave dielectric performances, sintering accelerator

I. Introduction

In the past decade, there have been considerable changes in the manufacturing of semi-conductors. To meet the needs of small-size and multifunctional chips (smaller, lighter, higher operating frequency), the technology for the production of multilayer circuits has attracted increasing attention. Low-temperature co-fired ceramics (LTCC) manufacturing technology is widely used in the production of multilayer chips because of its stable physical and electronic properties, easy production, and high-density chip packaging. Related wireless communication and military radar applications also use LTCC because of the need for high reliability and flexibility in research and development. In the field of wireless communications, as the operating frequency increases, the dielectric loss of traditional PCB production also increases, so LTCC is attracting considerable attention here, too. Therefore, to meet this demand, it is imperative to develop a low-temperature co-fired ceramic material system with low loss [1–4].

Dielectric ceramics are used in the field of microwave communication mainly because of their resistance to the influence of environmental factors (such as humidity, oxidation resistance, appropriate hardness, etc.), and, on the other hand, because of their high relative dielectric coefficient (ε_r) and magnetic permeability (μ). In addition, the size of the microwave component is proportional to $\lambda_0/\sqrt{(\varepsilon_r)}$, where λ_0 is the wavelength of the free space and ε_r is the dielectric constant of the dielectric ceramics, so to reduce the size of the microwave component, a substrate composition with a higher dielectric constant is selected [5–8].

Because $MgTiO_3$ (MT) has a very high quality factor, it has received a large amount of research investment, and its dielectric performances are $\varepsilon_r \sim 17$, a $Qf \sim 160\,000$ GHz, $\tau_f \sim$ -51 ppm/K [9–11]. In the past, to improve its dielectric performances, we used a partial substitution method, replacing magnesium with 0.05 mole cobalt, and achieved quite good results [$Mg_{0.95}Co_{0.05}TiO_3$ (MCT):ε_r of 16.8, Qf of 230 000 GHz, and τ_f of -54 ppm/K] [12–13]. However, because it still has the two disadvantages of negative temperature coefficients and high sintering temperature, the cost of component production does not meet industry needs. To compensate for the negative temperature characteristics, we used the mixing rule to mix MCT with compositions with ultra-high positive temperature coefficients (τ_f) (such as $CaTiO_3 \sim$ +800 ppm/K, $Ca_{0.6}La_{0.8/3}TiO_3 \sim$ +213 ppm/K, $Ca_{0.61}Nd_{0.78/3}TiO_3 \sim$ +270 ppm/K), and obtain temperature characteristics close to zero [12–15].

* Corresponding author: chshen0656@mail.mcu.edu.tw

In this study, we selected a mixture of $Mg_{0.95}Co_{0.05}TiO_3$ and $Ca_{0.61}Nd_{0.78/3}TiO_3$ (CNT) ceramic system and when the ratio of MCT and CNT is 9:1(9MCT-CNT) at 1 350 K/4 h, the microwave dielectric performances are $\varepsilon_r \sim 22.1$, a $Qf \sim 102\,000$ GHz, $\tau_f \sim -25.4$ ppm/K. To lower its sintering temperature, we referred to published works and selected materials with low melting points (B_2O_3, CuO, V_2O_5, ZnO) to observe the changes and characteristics of phase composition [16–21].

II. Experimental Procedure

High-purity chemical powders magnesium oxide (MgO), cobalt oxide (CoO), calcium carbonate ($CaCO_3$), neodymium oxide (Nd_2O_3), and titanium dioxide (TiO_2) were mixed according to the chemical composition ratio of $Mg_{0.95}Co_{0.05}TiO_3$ and $Ca_{0.61}Nd_{0.78/3}TiO_3$. The mixtures were ball-ground for 24 h, dried, and pre-phased at 1 100 °C for 4 h ($Mg_{0.95}Co_{0.05}TiO_3$), 3 h ($Ca_{0.61}Nd_{0.78/3}TiO_3$). Then, the pre-phased reagents were formulated again according to the chemical molar ratio of $0.9Mg_{0.95}Co_{0.05}TiO_3$ - $0.1\ Ca_{0.61}Nd_{0.78/3}TiO_3$ with varied types and contents of sintering accelerators (B_2O_3, CuO, V_2O_5, ZnO), and re-ground for 24 h. The mixtures, together with PVA (PVA 500; Showa, Tokyo, Japan) binder, were subsequently granulated and uniaxially pressed into pellets measuring 5 mm in thickness and 11 mm in diameter at 2 000 MPa. All samples were then sintered at 1 200 – 1 300 °C for 4 h. The subsequent phase identification of the specimens was conducted by means of X-ray pattern analysis using a Siemens D5000 diffractometer (XRD, Munich, Germany) with Cu-K_α radiation (at 40 kV and 40 mA). The XRD analysis of the sample was performed at a scan speed of 2 degrees/minute, with a step size of 0.06 degrees. The range of the 2 theta was set to 20 – 60 degrees. The XRD data analysis and the lattice constants calculation were performed using DIFFRAC software. The microstructures were studied using ultra-high-resolution scanning electron microscopy (SEM; Philips XL-40FEG, Eindhoven, Netherlands) equipped with energy dispersion spectroscopy (EDS). The densities were measured with the Archimedes method. ε_r and Qf values of the samples were measured using the Hakki-Coleman [22] and Courtney [23] methods on a vector network analyzer (HP8757D) and HP8350B sweep oscillator connections. The thermal coefficients (τ_f) of the samples were assessed by keeping the dielectric resonator (DR) inside a temperature-controlled stove with a temperature range of 20 °C to 80 °C. The τ_f can be calculated with the following equation:

$$\tau_f = (f_2 - f_1)/(T_2 - T_1)$$

where f_1 and f_2 represent the resonant frequencies at $T_1 = 20$ °C and $T_2 = 80$ °C, respectively.

III. Results and Discussion

Fig. 1 shows the XRD diffraction patterns recorded with 0.25-wt%-V_2O_5-added 9MCT-CNT ceramics sintered at varied sintering temperatures for 4 h. All the results showed that this is a two-phase system due to the structural dissimilarities, where the MCT ceramic (JCPDS #06 – 0494) is the principal phase with an ilmenite structure coexisting with the CNT ceramic (JCPDS #22 – 0153) as the secondary phase with a pseudo-cubic perovskite structure. In addition, in all experiments, a very small amount of secondary phase ($MgTi_2O_5$: JCPDS #82 – 1125) generation was still found. The main reasons are the increase in the possibility of secondary crystallization nucleation due to the uneven particle size of the initial powder, the increase in the activity rate of grain boundaries due to the high sintering temperature, or the local inhomogeneous liquid phase. In addition, when the proportion of magnesium oxide to titanium dioxide is 1:2, $MgTi_2O_5$ will form an intervening phase in the microstructure of the composition and cannot be completely removed [19, 24].

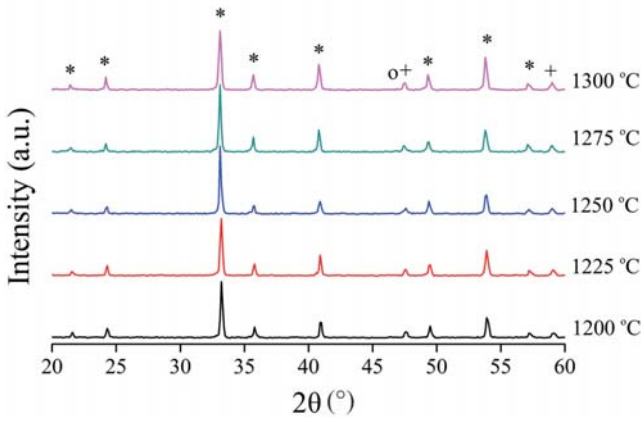

Fig. 1: The XRD results of 9MCT-CNT ceramics with 0.25 wt% V_2O_5 at varied phase-forming temperatures.

The lattice parameters and phase ratio of 9MCT-CNT ceramics with 0.25 wt% V_2O_5 at varied temperatures for 4 h are shown in Table 1. It can be seen in the table that because the sintering temperature rises, the particles grow, which in turn increases the proportion of MCT. The reason why the proportion of $MgTi_2O_5$ is very small may be that its optimal phase temperature has not been reached. In addition, due to structural differences, the lattice constant of MCT has not changed significantly as a result of the addition of CNT or accelerators.

The XRD diffraction patterns recorded with varied types and contents of sintering accelerators (B_2O_3, CuO, V_2O_5, ZnO) to the 9MCT-CNT ceramics are presented in Fig. 2. The phase formation of the 9MCT-CNT ceramics was not influenced by the different accelerators, but the secondary phase can still be observed and might affect the dielectric performance of the overall ceramic system [25]. The phase-forming temperature of the $MgTi_2O_5$ needs to be as high as 1 450 °C, so the higher the phase-forming temperature of the ceramic system, the more severe the influence of the $MgTi_2O_5$ [26]. The lattice parameters of 9MCT-CNT ceramics with varied types and contents of sintering accelerators at their optimal phase-forming temperatures for 4 h are shown in Table 2. All the results show that this is a multiphase ceramic system with MCT [JCPDS #06 – 0494, a = b = 5.054 (Å), c = 13.898 (Å)] as the main phase. When 0.05 moles of cobalt (Co^{2+}) replace magnesium (Mg^{2+}), because of the difference in ion radii between the two (Co: 0.82 Å, Mg: 0.78 Å), this will have a local slight effect on the lattice constant of $MgTiO_3$. When MCT is mixed with

Table 1: The lattice constants of 9MCT-CNT ceramics with 0.25 wt% V_2O_5 sintered at varied temperatures for 4 h. Each phase proportion is determined by all peak areas of XRD results.

9MCT-CNT - 0.25 wt V_2O_5					
S.T.	a	c	MT	CNT	MT2
1200	5.0618±0.0076(Å)	13.9169±0.0276(Å)	89.91	9.31	0.78
1225	5.0505±0.0114(Å)	13.8741±0.0413(Å)	90.23	9.01	0.76
1250	5.0524±0.0146(Å)	13.8911±0.0532(Å)	91.68	7.6	0.72
1275	5.0630±0.0076(Å)	13.9203±0.0277(Å)	91.17	8.05	0.77
1300	5.0517±0.0115(Å)	13.8773±0.0415(Å)	90.9	7.59	1.47

Table 2: The lattice constants of 9MCT-CNT ceramics with varied types and contents of sintering accelerators at their optimal phase-forming temperatures for 4 h. Each phase proportion is determined by all peak areas of XRD results.

9MCT-CNT- varied accelerators					
	a	c	MT	CNT	MT2
0.25 wt% B_2O_3	5.0529±0.0115(Å)	13.8804±0.0418(Å)	92.98	5.98	1.04
0.5 wt% B_2O_3	5.0417±0.0104(Å)	13.8609±0.0376(Å)	93.42	5.68	0.9
0.25 wt% CuO	5.0642±0.0077(Å)	13.9236±0.0279(Å)	89.72	9.3	0.98
0.5 wt% CuO	5.0642±0.0077(Å)	13.9236±0.0279(Å)	91.02	8.25	0.73
0.25 wt% V_2O_5	5.0524±0.0146(Å)	13.8911±0.0532(Å)	91.68	7.6	0.72
0.5 wt% V_2O_5	5.0517±0.0115(Å)	13.8773±0.0415(Å)	92.04	7.24	0.72
0.25 wt% ZnO	5.0473±0.0081(Å)	13.9332±0.0296(Å)	91.8	7.52	0.69
0.5 wt% ZnO	5.0411±0.0160(Å)	13.8473±0.0579(Å)	91.57	7.76	0.67

CNT, the lattice constant of the MCT is not affected because the structural differences and the ion radii of magnesium (0.78 Å) and cobalt (0.82 Å) are much smaller than that of calcium (1.06 Å) and neodymium (1.15 Å). This result is consistent with Fig. 1, the lattice constant of the MCT is not affected by the type and content of accelerators.

Fig. 3 shows the SEM micrographs of the 9MCT-CNT ceramics with 0.25 wt% CuO sintered at varied temperatures. In Figs. 3a and 3b, the particles are small, the pores are large and the structure is not dense. As the temperature rises from 1 200 °C to 1 250 °C, driven by thermal stress, the grains are connected and grow, so that the porosity decreases, the structure tends to be dense and the grain size is more consistent in Fig. 3c. However, when the temperature rises above 1 250 °C, the particle will show excessive growth owing to the extrusion between the particle and the air pressure as shown in Figs. 3d and 3e [27–29]. With the addition of varied accelerators, the resulting SEM results are almost identical. To further explore the composition ratio of grains in the structure, the EDS results of the SEM image represented in Figs. 3c and 3e for Spots A-C are shown in Table 3. Different grains can be distinguished; in Spot A is $Mg_{0.95}Co_{0.05}TiO_3$; Spot B is $Ca_{0.61}Nd_{0.78/3}TiO_3$ and Spot C is the secondary phase ($MgTi_2O_5$). The same result can be obtained from the analysis of EDS and XRD, which is a three-phase system.

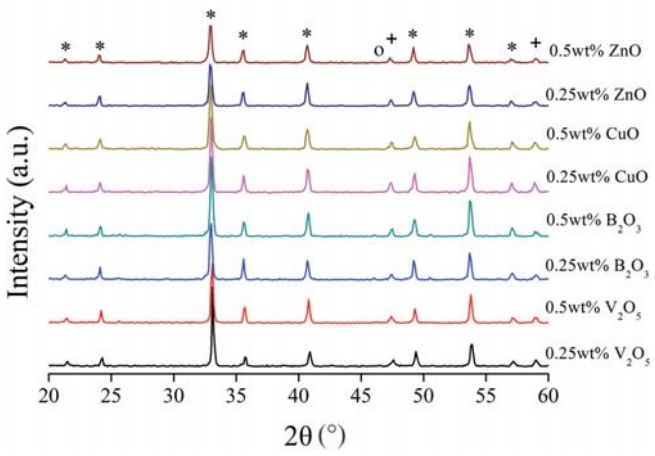

Fig. 2: The XRD results of 9MCT-CNT ceramics with varied types and contents of sintering accelerators at their optimal phase-forming temperatures.

The results for the density and permittivity ($\varepsilon_r$values) of the 9MCT-CNT ceramics with varied types and contents of sintering accelerators at varied temperatures are shown in Fig. 4. At 1 200 °C, the particles are small, porosity is large, and the density is lower because the thermal drive energy is insufficient. When the temperature rises to 1 250 °C, the thermal drive energy increases, driving the grain boundary to move and the grain to dissolve, so

that the grain grows, the grain size is more consistent, the porosity decreases, the overall structure tends to be dense, and the density increases. From the results of all types of accelerators, it can be seen that the phase-forming temperature is effectively reduced by about 100 °C (from 1 350 °C to 1 250 °C) due to liquid phase sintering. This is conducive to the dissolution between grains, recombinant grains, and wetting grain boundaries; so that the grain boundaries move more solution to achieve structural densification. Compared with the SEM in Fig. 3, at 1 200 °C, the density is lower due to the small particles and higher porosity. At 1 250 °C, the particle size is more consistent, the cavity is reduced due to grain expansion, and the density is enhanced. Therefore, when varied types of low-melting-point materials are added as sintering accelerators, liquid phase sintering of the 9MCT-CNT ceramics occurs. Typically, at the appropriate content of sintering accelerators, the phase-forming temperature can be effectively reduced. However, when the sintering accelerator content is superabundant, the grains grow immoderately, and with a larger particle size, the reorganization will be subject to greater resistance and there will be fewer pores in the boundary, meaning it is not easy to exclude the effect of porosity and other factors will influence the variation in the density and microwave dielectric performances. The ε_r values are quite sensitive to changes in temperature, which is the same as the trend towards density. According to the SEM results, the increase in temperature leads to grain growth, cavity shrinkage, and densification of the structure of 9MCT-CNT ceramics. The optimal dielectric performances obtained with the addition of varied types of sintering accelerators to 9MCT-CNT ceramics are listed in Table 4. It is known that the optimal phase-forming temperature for a single accelerator is 1 250 °C.

Table 3: The EDS results of particle formation for Spots A, B, and C in Figs. 3c and 3e.

	Atom (%)					
Spot	MgK	CoK	CaK	NdK	TiK	OK
A	28.11	3.21	0	0	34.36	34.32
B	0	0	16.89	8.81	26.84	47.46
C	12.96	0.62	0	0	23.35	63.07

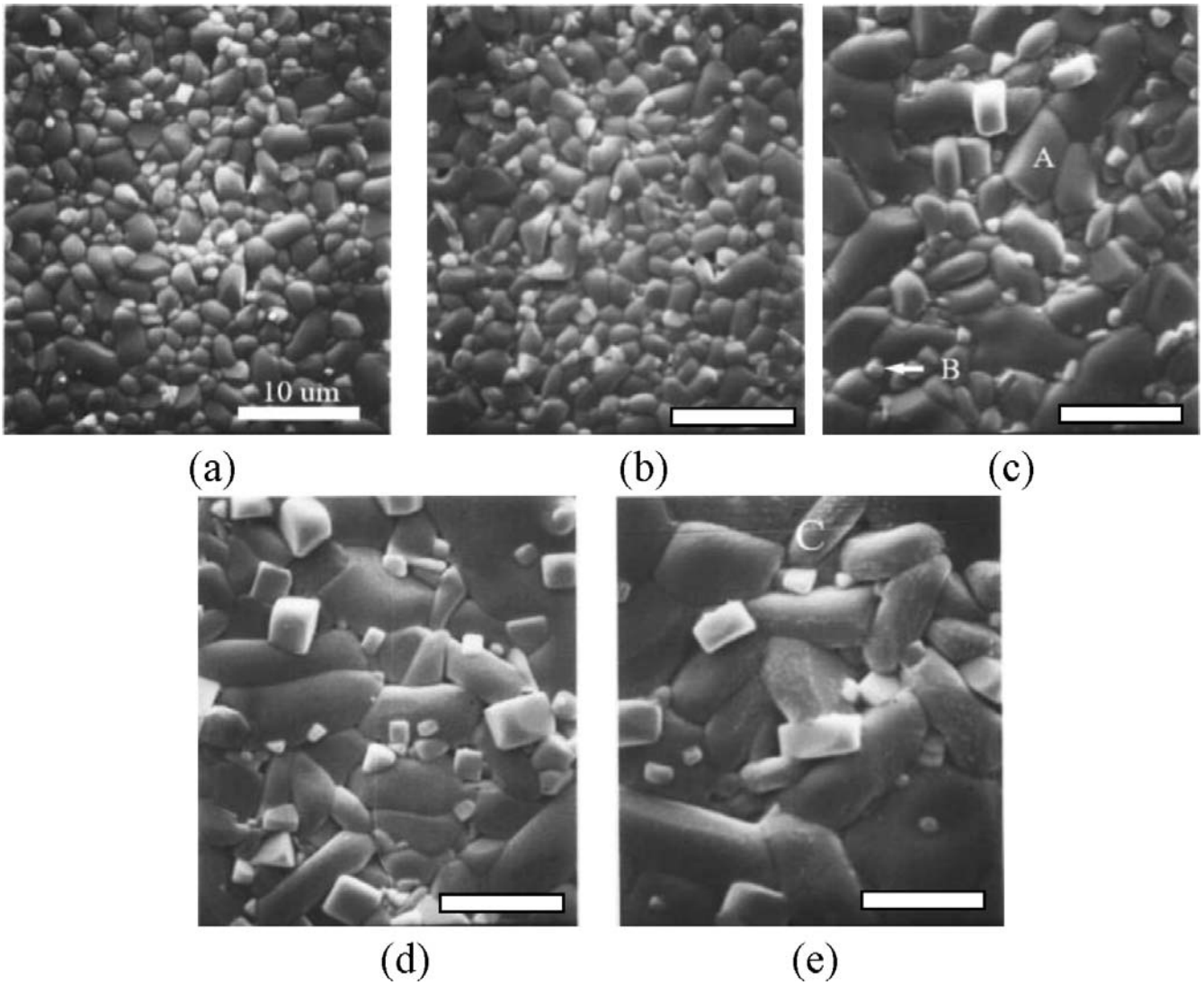

Fig. 3: The SEM images of 9MCT-CNT ceramics were obtained with 0.25 wt% CuO at (a) 1 200 °C, (b) 1 225 °C, (c) 1 250 °C, (d) 1 275 °C, (e) 1 300 °C for 4 h.

Table 4: The dielectric performances with varied types of sintering accelerators to 9MCT-CNT ceramics.

Accelerators	Content (wt%)	S.T.(°C)	D(g/cm^3)	ε_r	Qf(GHZ)	τ_f(ppm/K)
-	-	1350	3.96	22.1	102,000	-25.4
B_2O_3	0.25		3.76	21.6	55,000	-25.4
	0.5		3.75	21.5	54,000	-24.6
CuO	0.25		3.88	22.4	57,000	-24.7
	0.5	1250	3.86	22.3	54,000	-27
V_2O_5	0.25		4.0	21.7	71,000	-22.7
	0.5		3.98	21.6	62,000	-25.7
ZnO	0.25		3.9	22	52,000	-22
	0.5		3.95	22.1	57,000	-20

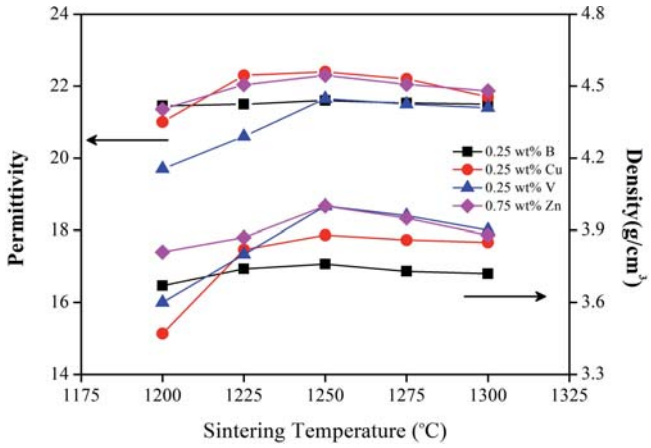

Fig. 4: The density and permittivity (ε_r values) of the 9MCT-CNT ceramics with varied types and contents sintering accelerators at varied temperatures.

Fig. 5 presents the quality factor (Qf value) and temperature characteristics (τ_f value) of the 9MCT-CNT ceramics with varied types and content of sintering accelerators at varied temperatures. The Qf value is the main reference index for dielectric ceramics in the field of microwave communication because the Qf value is proportional to the reciprocal of dielectric loss. In general, dielectric loss can be defined as the sum of intrinsic and extrinsic losses. The intrinsic loss is the loss of a perfect crystal, which depends on phonon motion and the action of the alternating electric field. Extrinsic losses are often associated with defects in the lattice structure, such as secondary phases, oxygen vacancy, uneven grain size, and excessive porosity [30–32]. Fig. 5 shows that the Qf value is also quite sensitive to changes in temperature. Therefore, it can be seen that density is not only related to the permittivity, but also has an effect on the Qf value. This is consistent with the results obtained with SEM. At 1 200 °C, the grains are smaller (phase not formed) and the pores are larger, so the density, permittivity (ε_r values), and Qf value are lower. At 1 250 °C, the particle size is more accordant (phase formed), the pores are shrunk and reduced, and the overall structure is the most densified owing to liquid phase sintering. When 9MCT-CNT ceramics with 0.25 wt% V_2O_5 are sintered at 1 250 K/4h, the optimal Qf value is 71 000 (GHz). When the temperature rises above 1 250 °C, a slight decrease in the Qf value can be observed, which may be due to excessive grain growth or secondary phase formation. Typically, the temperature characteristics (τ_f values) depend on the phase composition in the material system. In the (1-x) $Mg_{0.95}Co_{0.05}TiO_3$ - $xCa_{0.61}Nd_{0.78/3}TiO_3$ dielectric ceramic system, the positive τ_f values of the CNT(+270 ppm/K) are much higher than the negative τ_f values of the MCT(-54 ppm/K), so the change in the τ_f values depends on the content of the CNT. As can be seen from Fig. 5 and Table 4, the τ_f values of 9MCT-CNT ceramics do not change significantly as a result of the addition of a sintering accelerator. In addition, the generation of the second phase ($MgTi_2O_5$) does not affect the τ_f values of the MCT, because the τ_f values of the two are similar.

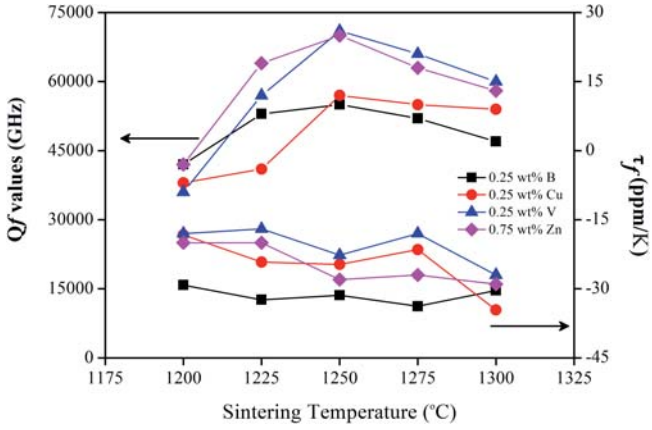

Fig. 5: Qf and τ_f values of the 9MCT-CNT ceramics with varied types and contents sintering accelerators at varied temperatures.

Table 4 shows the results of dielectric performances after adding varied types of sintering accelerators to 9MCT-CLT ceramics. With the addition of all types of accelerator, the phase-forming temperature can be effectively reduced. However, with the addition of accelerators, liquid phase sintering impairs the dielectric properties. When 9MCT-CNT ceramics with 0.25 wt% V_2O_5 are sintered at 1 250 K/4h, the optimal dielectric performances are obtained with an ε_r of 21.7, a Qf of 71 000 GHz, and a τ_f of -22.7 ppm/K.

IV. Conclusions

To eliminate two disadvantages of MCT, we mixed it with CNT to compensate for its negative temperature characteristics and added accelerators to reduce the phase-forming temperature. The additions with varied types (B_2O_3, CuO, V_2O_5, ZnO) and contents of sintering accelerators can effectively reduce the phase-forming temperature of 9MCT-CNT ceramics. Compared with undoped 9MCT-CNT ceramics, the composition after addition of the accelerator can reduce the phase-forming temperature by about 100 °C (from 1 350 °C to 1 250 °C). When a sintering accelerator was added, the generation of secondary phases ($MgTi_2O_5$) negatively affected the microwave dielectric performances, but not the temperature characteristics. The 9MCT-CNT ceramic with 0.25 wt% V_2O_5 sintered at 1 250 K/4h exhibited optimal microwave dielectric performances: a permittivity (ε_r) of 21.7, a *Qf* of 71 000 (GHz), and a τ_f value of -22.7 ppm/K. These results make MCT more suitable for the production of microwave communication components.

References

1 Zhu, S.K. et al.: 5G microstrip patch antenna and microwave dielectric properties of 4 mol%LiF-MgO-xwt%$MTiO_3$ (M = Ca, Sr) composite ceramics, *J. Mater. Sci. Mater Electron.*, **32**, [19], 23880 (2021).

2 Antipov, O.L., Novikov, A.A., Eranov, I.D.: In Proceedings of the 2014 Int. Conf. Laser Optics, St. Petersburg, Russia, (2014).

3 Jang, Y., Kim, J., Kim, S.: Design and fabrication of a compact 3-dimensional stacked type dielectric ceramic waveguide bandpass filter, *IEEE Microw. Wirel. Common. Lett.*, **24**, 665 – 667, (2014).

4 Paul, M.C., Dhar, A., Das, S.: *IEEE Photonics*, **7**, 1 – 7 (2015).

5 Palmero, P.: Structural ceramic Nanocomposites: A review of properties and Powders' synthesis methods, *Nanomaterials*, **5**, 656 – 696, (2015).

6 Penn, S.J., Alford, N.M.: Effect of porosity and grain size on the microwave dielectric properties of sintered alumina, *J. Am. Ceram. Soc.*, **80**, 1885 – 1888, (1997).

7 Kretly, L.C., Almeida, A.F.L., Fechine, P.B.A.: Dielectric permittivity and loss of $CaCu_3Ti_4O_{12}$ (CCTO) substrates for microwave devices and antennas, *J. Mater. Sci. Mater. Electron.*, **15**, 657 – 663, (2004).

8 Tang, B., Xiang, Q., Fang, Z.X.: Influence of Cr3+ substitution for Mg2+ on the crystal structure and microwave dielectric properties of CaMg1-xCr2x/3Si_2O6 ceramics, *Ceram. Int.*, **45**, 11484 – 11490, (2019).

9 Sohn, J.H., Inaguma, Y., Yoon, S.O.: Microwave dielectric characteristics of ilmenite-type titanates with high Q values, *Jpn. J. Appl. Phys.*, **33**, 5466, (1994).

10 Wakino, K.: Recent development of dielectric resonator materials and filters in japan, *Ferroelectrics,* **91**, 69 – 86, (1989).

11 Yuan, S., Gan, L., Ning, F.: High-Q×f 0.95 $MgTiO_3$-0.05 $CaTiO_3$ microwave dielectric ceramics with the addition of LiF sintered at medium temperatures, *Ceram. Int.*, **44**, 20566 – 20569, (2018).

12 Huang, C.L., Pan, C.L.: Dielectric properties of (1-x)($Mg_{0.95}Co_{0.05}$) TiO_3-x$CaTiO_3$ ceramic system at microwave frequency, *Mater. Res. Bull.*, **37**, 2483 – 2490, (2002).

13 Huang, C.L., Shen, C.H.: Dielectric properties and applications of low loss (1-x)($Mg_{0.95}Co_{0.05}$) TiO_3-x$Ca_{0.8}Sm_{0.4/3}TiO_3$ ceramic system at microwave frequency, *J. Alloy. Compd.*, **468**, 516 – 521, (2009).

14 Shen, C.H., Pan, C.L.: Structure, dielectric properties, and applications of ($Na_{0.5}Sm_{0.5}$) TiO_3-modified ($Mg_{0.95}Ni_{0.05}$) TiO_3 ceramics at microwave frequency, *Mater. Res. Bull.*, **65**, 169 – 174, (2015).

15 Ullah, A., Iqbal, Y., Mahmood, T.: Kinetic analysis on the synthesis of $Mg_{0.95}Zn_{0.05}TiO_3$ microwave dielectric ceramic by polymeric precursor method, *Ceram. Int.*, **41**, 15089 – 15096, (2015).

16 Huang, C.L., Pan, C.L., Shen, C.H.: *J. Mater. Sci.*, **21**, 149 – 151 (2002).

17 Fu, Z.F., Chen, X.Y., Yang, Z.Y.: Enhanced temperature stability of Mg_2TiO_4-based ceramics by LCB additive and temperature-stable characterization, *Ceram. Int.*, **48**, 36638 – 36643, (2022).

18 Shen, C.H., Huang, C.L.,: Characterization and dielectric behavior of B_2O_3-doped 0.9 $Mg_{0.95}Co_{0.05}TiO_3$-0.1 $Ca_{0.6}La_{0.8/3}TiO_3$ ceramic system at microwave frequency, *J. Alloy. Compd.*, **504**, 228 – 232, (2010).

19 Zhifen, F., Yubin, S., Zhongyi, Y.: Novel temperature-stable $MgTi_{0.95}Sn_{0.05}O_3$-based microwave dielectric ceramics, *Integrated Ferroelectrics*, **231**, 98 – 105, (2023).

20 Yu, H., Luo, T.: Recent advances in joining of SiC-based materials (monolithic SiC and SiC_f/SiC composites): joining processes, joint strength, and interfacial behavior, *J. Adv. Appl. Ceram.*, **118**, 98 – 105, (2019).

21 Pan, C.L., Shen, C.H.: The enhanced phase-forming capacity of (1-x)$Mg_{0.95}Co_{0.05}TiO_3$-x$Ca_{0.6}La_{0.8/3}TiO_3$ dielectric ceramics modified using multiple sintering aids, *Crystals*, **13**, [6], 927, (2023).

22 Hakki, B.W., Coleman P.D.: A dielectric resonator method of measuring inductive capacities in the millimeter range, *IRE Trans. Microwave Theory Tech.*, **8**, 402 – 410, (1960).

23 Courtney, W.E.: Analysis and evaluation of a method of measuring the complex permittivity and permeability microwave insulators, *IEEE Trans. Microwave Theory Tech.*, **18**, 476 – 485, (1970).

24 Liao, J., Senna, M.: Crystallization of titania and magnesium titanate from mechanically activated $Mg(OH)_2$ and TiO_2 gel mixture, *Mater. Res. Bull.*, **30**, 385, (1995).

25 Silverman, B.D.: Microwave absorption in cubic strontium titanate, *Phys. Rev.*, **125**, 1921, (1962).

26 Huang, C.L., Shen, C.H.: Phase evolution and dielectric properties of ($Mg_{0.95}M_{0.05}^{2+}$)Ti_2O_5 (M^{2+}=Co, ni, and Zn) ceramics at microwave frequencies, *J. Am. Ceram. Soc.*, **92**, 384, (2009).

27 Huang, C.L., Liu S.S.: Dielectric characteristics of the (1-x) Mg_2TiO4-x$SrTiO_3$ ceramic system at microwave frequencies, *J. Alloy. Compd.*, **471**, L9 – L12, (2009).

28 Huang, C.L., Liu, S.S.: Dielectric properties of a new ceramic system ($Mg_{0.95}Zn_{0.05}$)$_2TiO_4$-$CaTiO_3$ at microwave frequencies, *Jpn. J. Appl. Phys.*, **48**, 071402, (2009).

29 Shen, C.H., Pan, C.L.,: Dielectric properties and applications of low-loss (1-*x*)($Mg_{0.95}Ni_{0.05}$)$_2TiO_4$-x$SrTiO_3$ ceramic system at microwave frequency, *Int. J. Appl. Ceram. Technol.*, **12**, E127 – E133 (2015).

30 Gurevich, G.L., Tagantsev, A.K.: Microwave ceramics for resonators and filters, *Low temperature. Sov. Phys. JETP*, **64**, 142 – 151, (1986).

31 Gurevich, G.L., Tagantsev, A.K.: Intrinsic dielectric loss in crystals, *Adv. Phys.*, **40**, 719 – 767, (1991).

32 Kajfezz, D., Guillon, P., Tucker, G.A. USA; pp. 10 – 62 (1998).